Preparation of N&O-doping and microporous carbon granules for effective CH$_4$ adsorption and separation from low-concentration coal-bed methane

Yao Li[a], Xiaohua Wang[a], Lanyun Wang[c], Ran Xu[b]*, Binbin Wang[d]*

[a] School of Safety Science and Engineering, Henan Polytechnic University, Jiaozuo, Henan 454000, China

[b] School of Safety and Management Engineering, Hunan Institute of Technology, Hengyang 421002, China

[c] School of Safety Science and Engineering, Changzhou University, Changzhou 213164, China

[d] School of Materials Science and Engineering, Henan Polytechnic University, Jiaozuo, Henan 454000, China

* Corresponding authors.

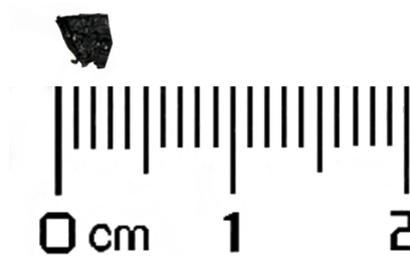E-mail addresses: rxu@hnit.edu.cn (R. X.); wangbb@hpu.edu.cn. (B.W.)

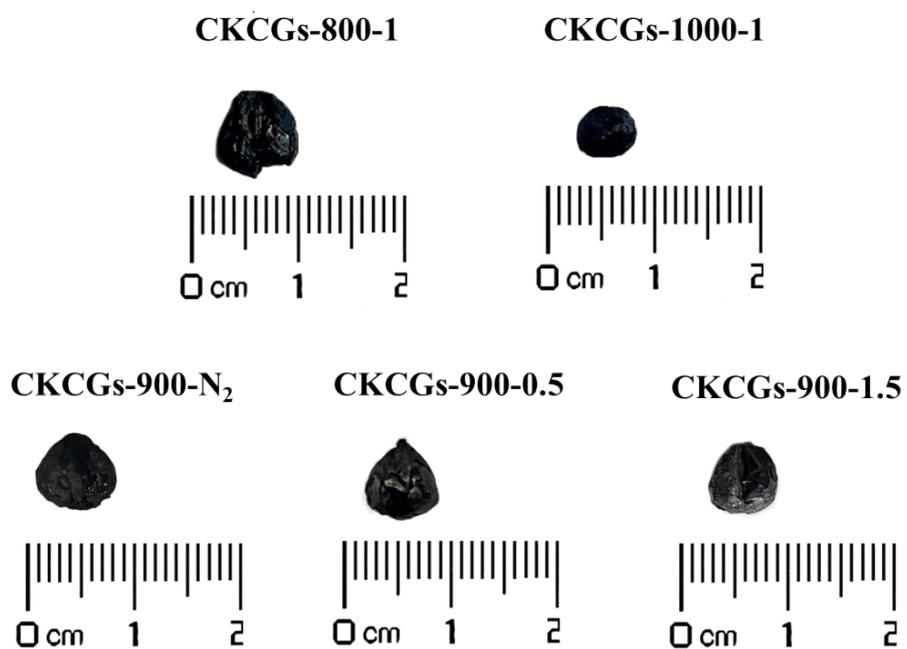**Fig. S1.** Photograph of CKCGs-900-1 hydrothermal 2 h.

Fig. S2. Photographs of CKCGs-800-1, CKCGs-900-N$_2$, CKCGs-900-0.5, CKCGs-900-1.5, and CKCGs-1000-1.
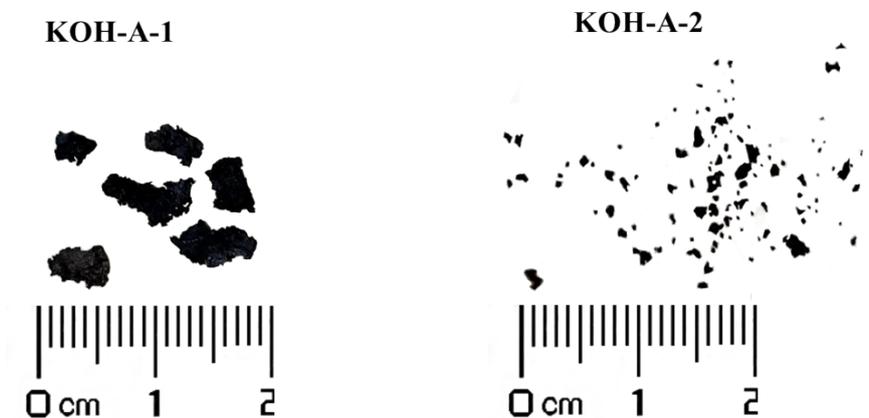

Fig. S3. Photographs of the KOH-A-1 and KOH-A-2

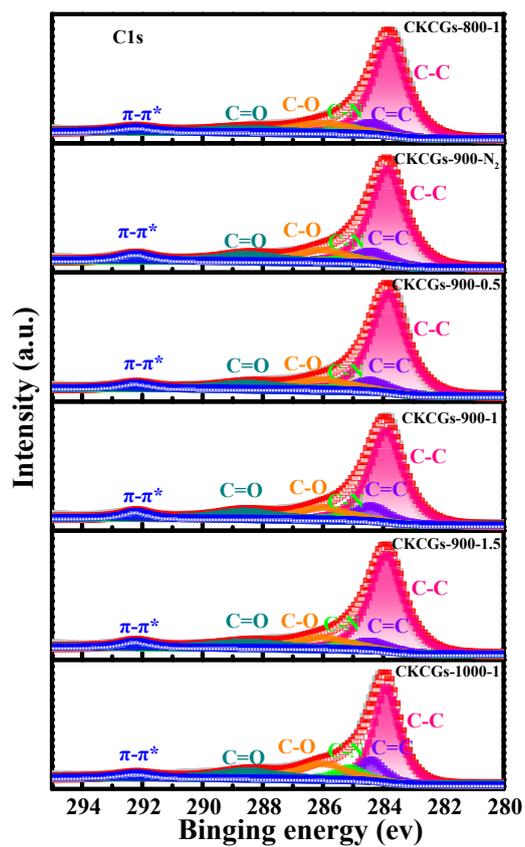**Fig. S4.** High-resolution XPS spectra of C1s for CKCGs.
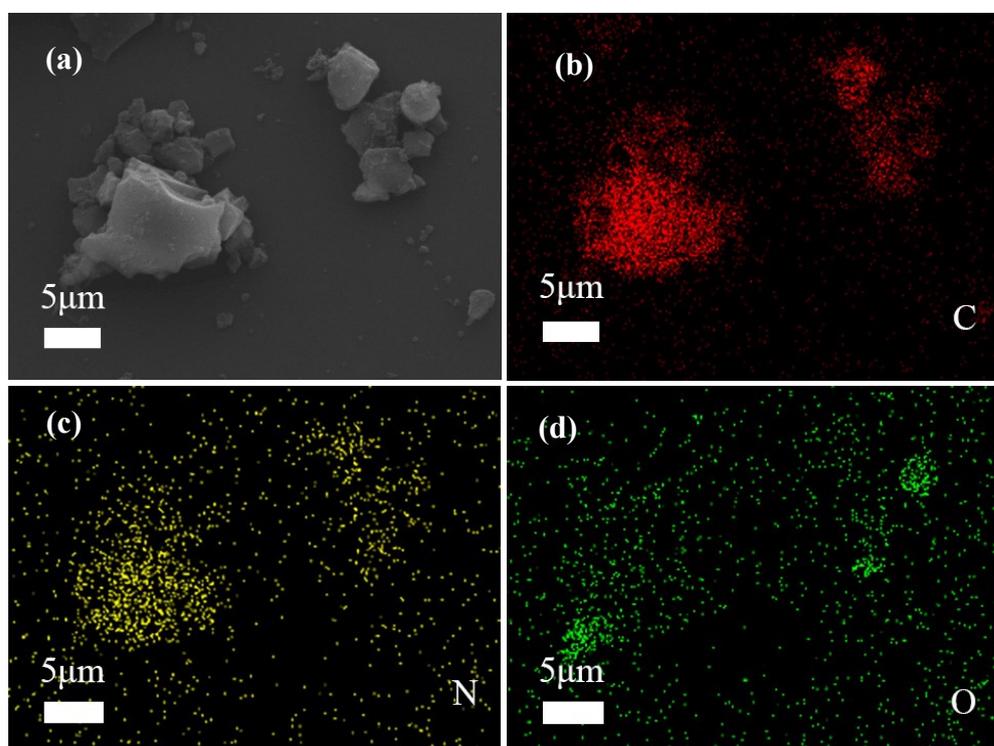

Fig. S5. (a) SEM image of CKCGs-900-1, and EDS elemental mapping images of (b) C, (c) N, and (d) O in CKCGs-900-1.
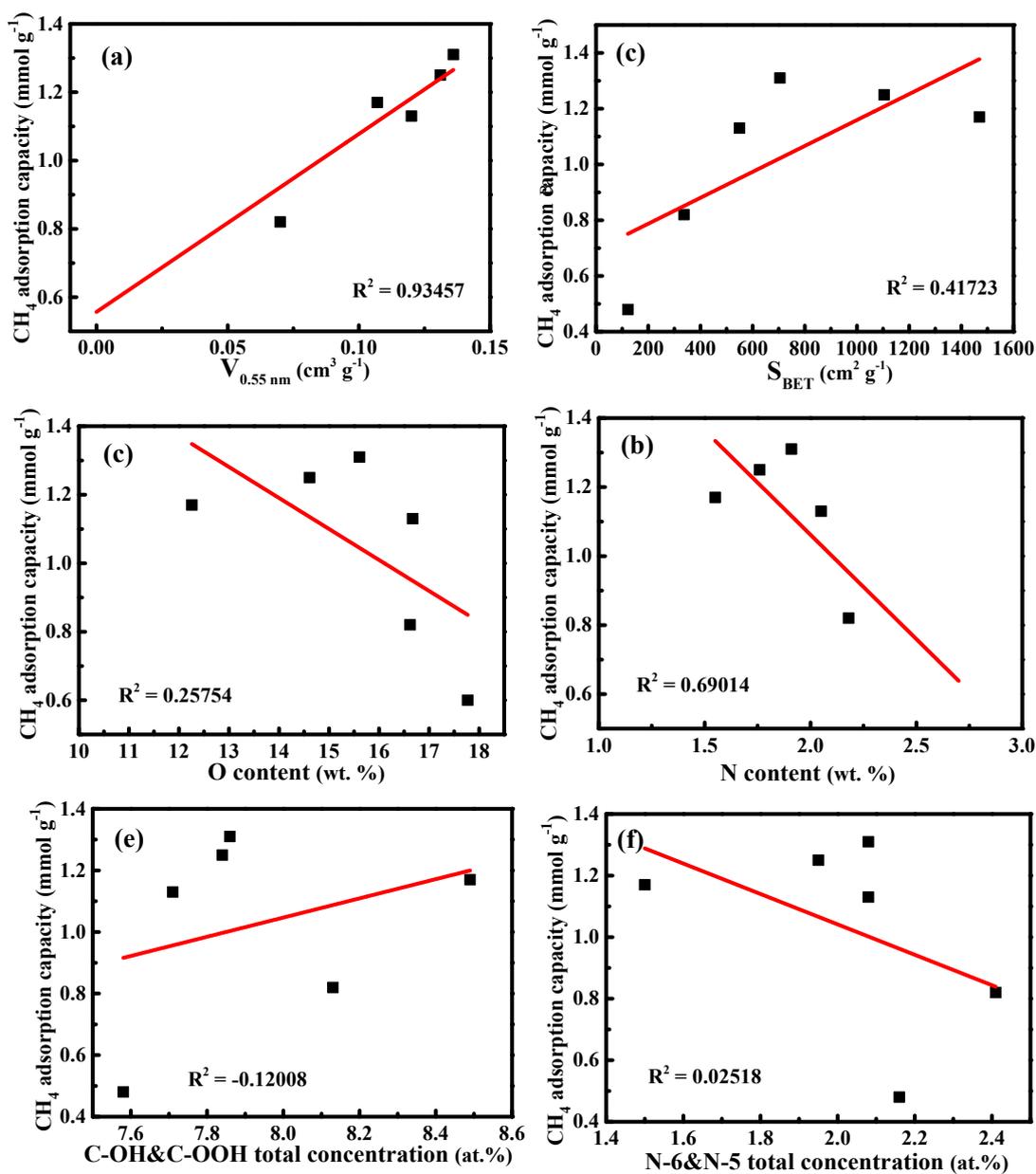
Fig. S6. The relationship of CH$_4$ adsorption capacity with (a) V$_{0.55\ nm}$, (b) S$_{BET}$, (c) O-content, (c) N-content, (e) surface C-OH&C-OOH total concentration and (f) surface N-5&N-6 total concentration.
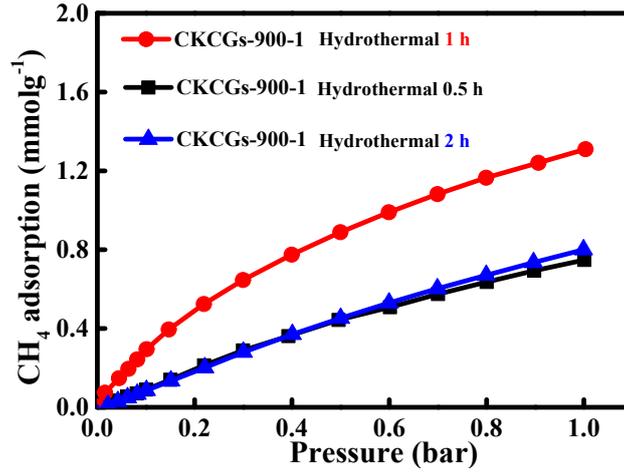
Fig. S7. Different hydrothermal duration affecting the CH$_4$ adsorption capacity. (Red marking hydrothermal 1 h, black marking hydrothermal 0.5 h, blue marking hydrothermal 2 h)
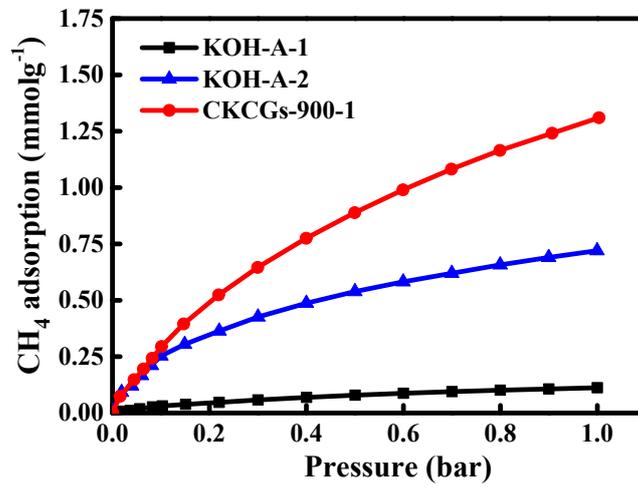
Fig. S8. CH$_4$ adsorption performance comparison of CKCGs-1, KOH-A-1 and KOH-A-2 at 25 °C and 1 bar.
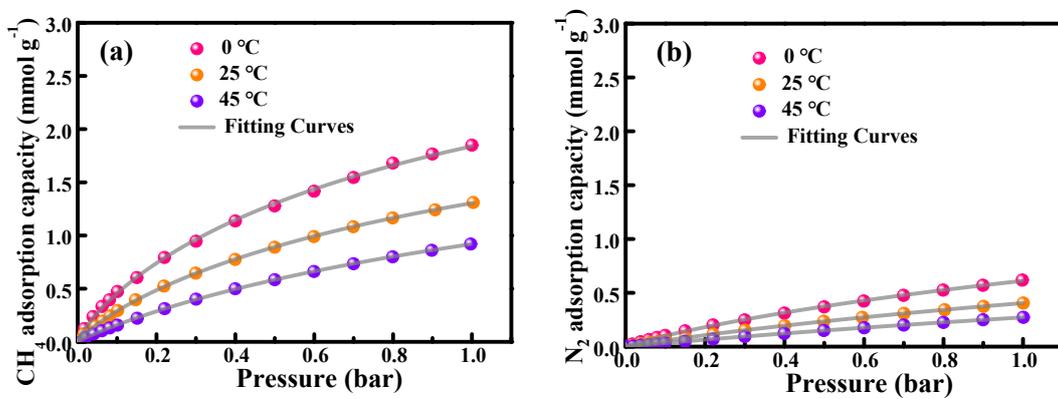
Fig. S9. The adsorption isotherms of (a) CH$_4$ and (b) N$_2$ on CKCGs-900-1 at 0, 25, and 45°C.
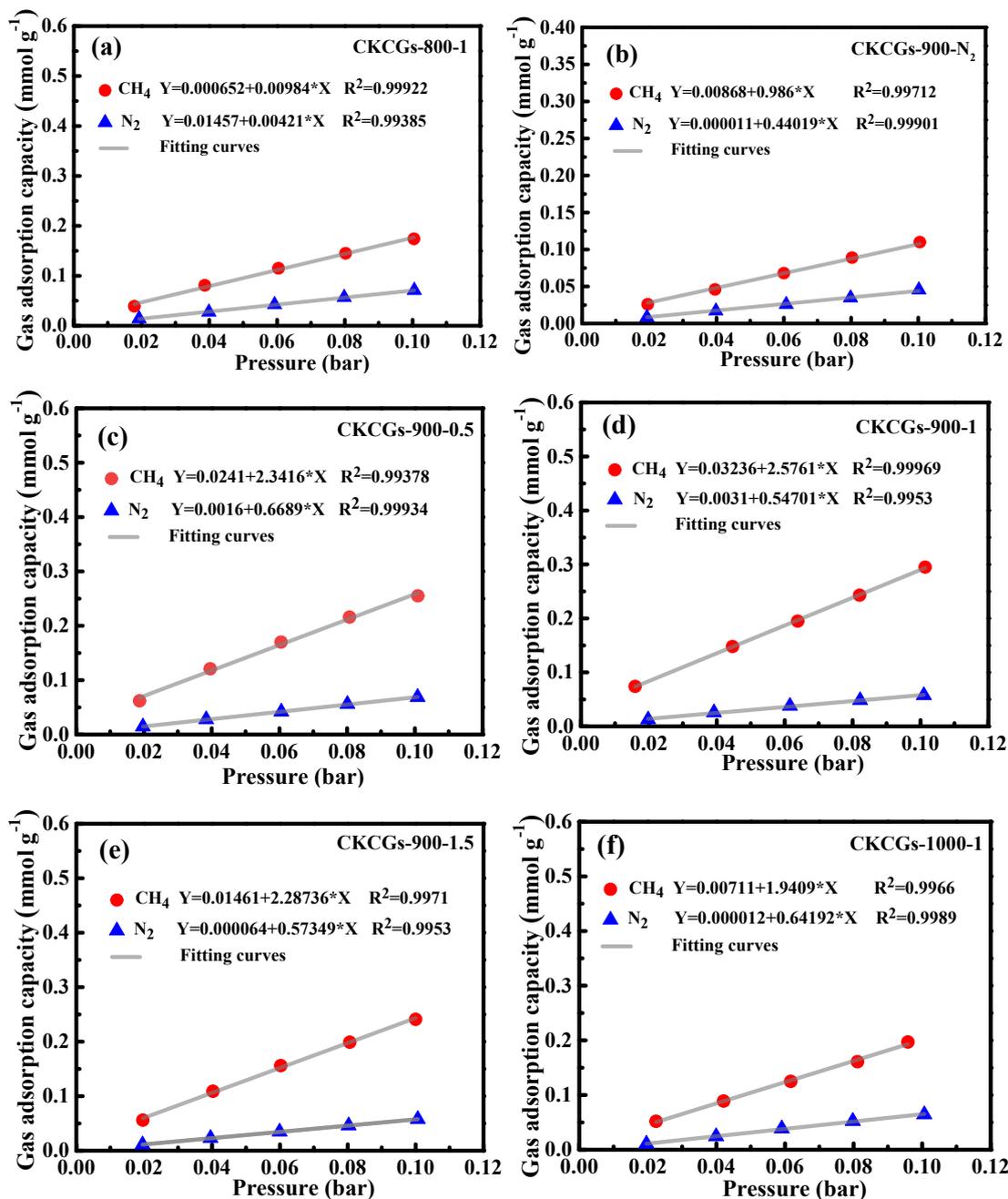
Fig. S10. The initial slopes of CH_4 and N_2 adsorption isotherms (0-0.12 bar) for (a) CKCGs-800-1, (b) CKCGs-900-0, (c) CKCGs-9-0.5, (d) CKCGs-900-1, (e) CKCGs-900-1.5 and (f) CKCGs-1000-1, at 25 °C.
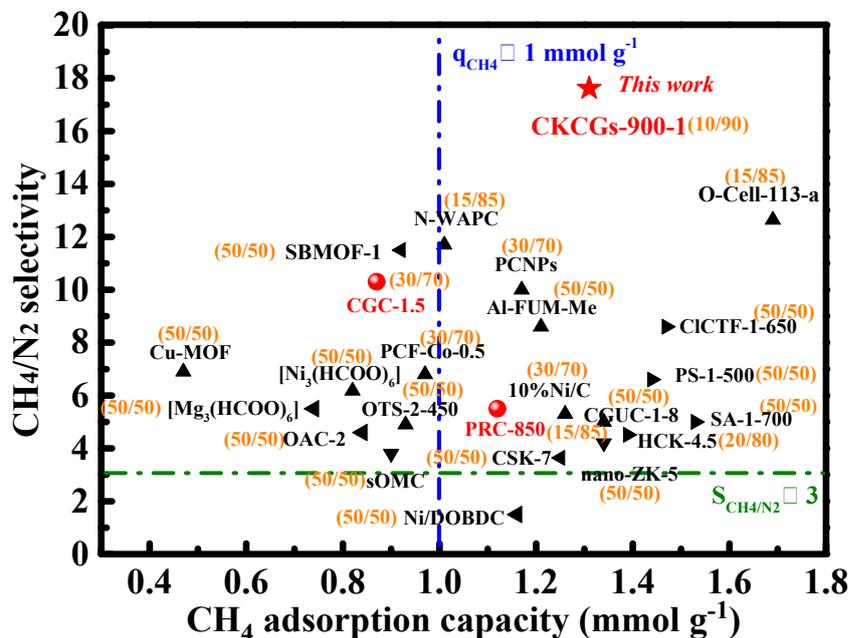
Fig. S11. Comparison of CH_4/N_2 selectivity and CH_4 adsorption capacity with some other adsorbents at 1 bar and 25 °C (red symbols present particle and column samples, black symbols represent powder samples, the orange values annotate the CH_4/N_2 proportion).
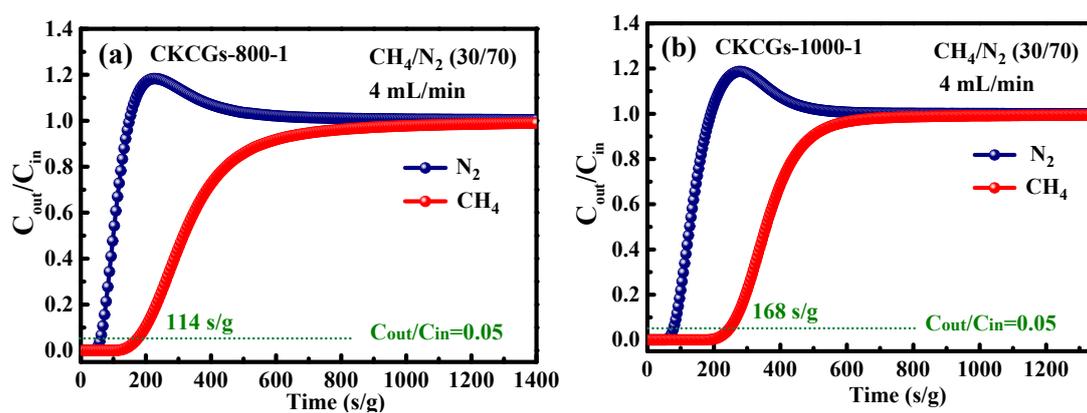
Fig. S12. Breakthrough curves for CH_4/N_2 (30/70 v/v) binary mixture on (a) CKCGs-800-1, (b) CKCGs-1000-1 at 25 °C and 1 bar.

Table S1. The mechanical strength and yield of these granular carbon samples.

Samples	Mechanical strength (N/granule)	Yields [a] (%)
CKCGs-800-1	25.95	21.07
CKCGs-900-N$_2$	37.18	16.13
CKCGs-900-0.5	31.07	19.24
CKCGs-900-1	21.61	17.57
CKCGs-900-1.5	12.03	13.85
CKCGs-1000-1	11.66	12.80

[a] Calculated by considering the mass change of the original precursor (corn kernels) upon the final obtained carbon granules.

Table S2. Average particle size and Standard Deviation of Corn Kernels and the derived carbon granules.

| Samples	Corn kernel size (cm)	carbon granule size (cm)					
		CKCGs-900-N$_2$	CKCGs-800-1	CKCGs-900-0.5	CKCGs-900-1	CKCGs-900-1.5	CKCGs-1000-1
No. 1	0.9	0.75	0.80	0.71	0.7	0.62	0.50
No. 2	0.91	0.78	0.79	0.72	0.68	0.65	0.48
No. 3	0.86	0.76	0.81	0.69	0.69	0.64	0.49
No. 4	0.91	0.75	0.82	0.71	0.71	0.59	0.51
No. 5	0.9	0.74	0.79	0.69	0.69	0.60	0.48
No. 6	0.88	0.76	0.81	0.68	0.68	0.61	0.52
No. 7	0.87	0.74	0.82	0.73	0.68	0.62	0.49
No. 8	0.89	0.75	0.78	0.73	0.7	0.63	0.50
No. 9	0.88	0.76	0.84	0.74	0.68	0.62	0.51
No. 10	0.92	0.77	0.82	0.70	0.73	0.59	0.48
No. 11	0.91	0.75	0.81	0.71	0.71	0.64	0.49
No. 12	0.89	0.74	0.80	0.69	0.67	0.62	0.49
Average particle size	0.89	0.75	0.82	0.71	0.70	0.61	0.49
Standard deviation	0.018	0.013	0.018	0.018	0.017	0.019	0.013

Table S3. Content of different O-containing functional groups in O1s spectra of CKCGs samples.

Samples	O/at. (%)	O groups ratio [b] (%)				O groups ratio [c]			
		C=O	C-OH	-COOH	O_2/H_2O	C=O	C-OH	-COOH	O_2/H_2O
CKCGs-800-1	14.92	43.29	47.62	6.93	2.16	6.46	7.10	1.03	0.33
CKCGs-900-N_2	15.04	47.54	49.18	1.23	2.05	7.15	7.40	0.18	0.31
CKCGs-900-0.5	14.46	43.54	45.80	7.51	3.15	6.30	6.62	1.09	0.45
CKCGs-900-1	14.33	41.35	46.41	8.44	3.80	5.93	6.65	1.21	0.54
CKCGs-900-1.5	14.00	41.17	47.32	8.71	2.80	5.76	6.62	1.22	0.40
CKCGs-1000-1	13.09	31.03	48.97	15.86	4.14	4.06	6.41	2.08	0.54

[a] The surface total O concentration (at.%) obtained from XPS analysis;

[b] Percentage of each deconvoluted peak in relation to O1s total area (%);

[c] The surface concentration (at.%) of each O-containing group is calculated by multiplying the percentage of deconvolution peak of each O group in the O1s spectra by the total O concentration. In the case of CKCG-900-1, for example, the C-OH percentage in O1s spectra of 46.41 % multiplied by the O content of 14.33 at. % is calculated to be 6.65 at. %.

Table S4. Content of different N-containing functional groups in O1s spectra of CKCGs samples.

Samples	N/at. (%)	N species ratio [b] (%)				N species ratio [c]			
		N-6	N-5	N-Q	N-X	N-6	N-5	N-Q	N-X
CKCGs-800-1	2.41	31.72	57.27	6.17	4.84	0.76	1.38	0.15	0.12
CKCGs-900-N_2	2.42	31.22	57.71	6.81	4.26	0.76	1.40	0.16	0.10
CKCGs-900-0.5	2.33	30.45	58.77	6.13	4.65	0.71	1.37	0.14	0.11
CKCGs-900-1	2.31	29.67	60.28	5.74	4.31	0.69	1.39	0.13	0.10
CKCGs-900-1.5	2.14	27.50	63.50	5.00	4.00	0.59	1.36	0.11	0.08
CKCGs-1000-1	1.81	18.09	64.82	9.55	7.54	0.33	1.17	0.17	0.14

[a] The surface total N concentration (at. %) obtained from XPS analysis;

[b] Percentage of each deconvoluted peak in relation to N1s total area (%);

[c] The surface concentration (at.%) of each N-containing group is calculated by multiplying the percentage of deconvolution peaks of each N group in the N1s spectra by the total N concentration. In the case of CKCG-900-1, for example, the N-5 percentage in N1s spectra of 60.28 % multiplied by the N content of 2.31 at. % is calculated to be 1.39 at. %.

Table S6. The comparison between CKCGs-900-1 and other representative adsorbents on CH_4 adsorption capacity and CH_4/N_2 IAST selectivity at 25 °C and 1 bar.

Adsorbent	Physical form	CH_4 uptake (mmol g^{-1})	CH_4/N_2 IAST Selectivity	Ratio of CH_4/N_2	Ref.
		@ 25 °C, 1 bar			
HCK4.5	Powdery	1.39	4.51	20/80	[S1]
Al-FUM-Me	Powdery	1.21	8.60	50/50	[S2]
SBMOF-1	Powdery	0.92	11.5	50/50	[S3]
nano-ZK-5	Powdery	1.34	4.2	20/80	[S4]
SA-1-700	Powdery	1.53	5.00	50/50	[S5]

Table S5. Langmuir-Freundlich parameters for the CH_4 and N_2 adsorption isotherms on the porous carbon granules.

Samples	Gas	Temperature	q_m	b	n	R^2
CKCGs-800-1	CH_4	25 °C	2.56065	0.39922	1.23015	0.99990
	N_2	25 °C	2.29363	0.14119	1.21101	0.99963
CKCGs-900-N_2	CH_4	25 °C	2.34149	0.21258	1.13587	0.99957
	N_2	25 °C	2.10798	0.13734	1.2235	0.99413
CKCGs-900-0.5	CH_4	25 °C	3.00275	0.54049	1.21938	0.99996
	N_2	25 °C	2.22188	0.17667	1.16042	0.99988
CKCGs-900-1	CH_4	0 °C	4.0012	0.8210	1.21851	0.99983
		25 °C	3.05675	0.70716	1.17389	0.99988
		45 °C	2.49156	0.56251	1.0713	0.99981
	N_2	0 °C	2.36322	0.30752	1.12021	0.99968
		25 °C	1.89563	0.24963	1.06393	0.99996
		45 °C	1.67176	0.18734	1.02128	0.99996
CKCGs-900-1.5	CH_4	25 °C	3.59313	0.47987	1.14975	0.99995
	N_2	25 °C	1.94714	0.26263	1.04394	0.99993
CKCGs-1000-1	CH_4	25 °C	3.5588	0.44928	1.10175	0.99983
	N_2	25 °C	2.6300	0.16395	1.09866	0.99981

N-WAPC	Powdery	1.01	11.76	15/85	[S6]
ClCTF-1-650	Powdery	1.47	8.60	50/50	[S7]
PS-1-550	Powdery	1.44	6.60	50/50	[S8]
sOMC	Powdery	0.90	3.80	50/50	[S9]
$[Ni_3(HCOO)_6]$	Powdery	0.82	6.18	50/50	[S10]
PCNPs	Powdery	1.17	10.0	30/70	[S11]
CSK-7	Powdery	1.25	3.64	50/50	[S12]
Cu-MOF	Powdery	0.47	6.9	50/50	[S13]
CGUC-1-8	Powdery	1.34	5.0	50/50	[S14]
PCF-Co-0.5	Powdery	0.97	6.8	30/70	[S15]
O-Cell-113-a	Powdery	1.69	12.64	15/85	[S16]
10 %Ni/C	Powdery	1.26	5.3	30/70	[S17]
OTS-2-450	Powdery	0.93	4.9	50/50	[S18]
OAC-2	Powdery	0.84	4.6	50/50	[S19]
Ni/DOBDC	Powdery	~1.16	~1.5	50/50	[S20]
$[Mg_3(HCOO)_6]$	Powdery	0.74	5.5	50/50	[S21]
Na-CHA-4.0	Powdery	1.34	-------	------	[S22]
PAF-1-SO$_3$H	Powdery	0.62	-------	-------	[S23]
PRC-850 binder-free	Shaped	1.12	5.5	15/85	[S24]
KOH0.5TP50 binder-containing	Shaped	1.459	-------	-------	[S25]
ACB-5 binder-containing	Shaped	1.125	-------	-------	[S26]
ACB-2 binder-containing	Shaped	1.094	-------	-------	[S26]
CGC-1.5 binder-containing	Shaped	0.87	10.3	30/70	[S27]
CKCGs-900-1	Granule	1.31	17.62	10/90	*this work*
CKCGs-900-1	Granule	1.31	11.59	15/85	*this work*
CKCGs-900-1	Granule	1.31	5.21	30/70	*this work*
CKCGs-900-1	Granule	1.31	2.40	20/50	*this work*

References

[S1] H. Lian, Y. Q. Zhao, L. P. Wang, Y. Wang, G. J. Zhang, Y. F. Zhang, Low-corrosion preparation of porous carbons with narrow micropores for efficient separation of CH$_4$/N$_2$, Mater. Today. Commun. 39 (2024) 108818.

[S2] M. Chang, T. G. Yan, Y. Wei, J. X. Wang, D. H. Liu, J. F. Chen, Enhancing CH$_4$ Capture from Coalbed Methane through Tuning van der Waals Affinity within Isoreticular Al-Based Metal-Organic Frameworks, ACS Appl. Mater. Interfaces. 14 (2022) 25374−25384

[S3] M. Chang, J. H. Ren, Q.Y. Yang, D. H. Liu, A robust calcium-based microporous metal-organic framework for efficient CH_4/N_2 separation, Chem. Eng. J. 408 (2021) 127294.

[S4] J. F. Yang, X. Tang, J. Q. Liu, J. Wang, H. Shang, L. G. Wu, J. P. Lia, S. G. Deng, Down-sizing the crystal size of ZK-5 zeolite for its enhanced CH4adsorption and CH_4/N_2 separation performances, Chem. Eng. J. 406 (2021) 126599.

[S5] F.Q. Yang, J. Wang, L. Liu, P.X. Zhang, W.K. Yu, Q. Deng, Z.L. Zeng, S.G. Deng, Synthesis of porous carbons with high N-content from shrimp shells for efficient CO_2-capture and gas separation, ACS Sustainable Chem. Eng. 6 (2018) 15550-15559.

[S6] Y. Li, R. Xu, B.B. Wang, J.P. Wei, L.Y. Wang, M.Q. Shen, J. Yang, Enhanced N-doped porous carbon derived from KOH-activated waste wool: A promising material for selective adsorption of CO_2/CH_4 and CH_4/N_2, Nanomaterials. 9 (2019) 266.

[S7] K.X. Yao, Y.L. Chen, Y. Lu, Y.F. Zhao, Y. Ding, Ultramicroporous carbon with extremely narrow pore distribution and very high nitrogen doping for efficient methane mixture gases upgrading, Carbon 122 (2017) 258-265.

[S8] F. Liu, Y. Zhang, P.X. Zhang, M. Xu, T. Tan, J. Wang, Q. Deng, L.Y. Zhang, Y.Q. Wan, S.G. Deng, Facile preparation of N and O-rich porous carbon from palm sheath for highly selective separation of $CO_2/CH_4/N_2$ gas-mixture, Chem. Eng. J. 399 (2020) 125812.

[S9] B. Yuan, X.F. Wu, Y.X. Chen, J.H. Huang, H.M. Luo, S.G. Deng, Adsorption of CO_2, CH_4, and N_2 on ordered mesoporous carbon: Approach for greenhouse gases capture and biogas upgrading, Environ. Sci. Technol. 47 (2013) 5474-5480.

[S10] Y. Guo, J. L. Hua, X. W. Liu, T. J. Sun, S. S. Zhao, S. D. Wang, Scalable solvent-free preparation of $[Ni_3(HCOO)_6]$ frameworks for highly efficient separation of CH_4 from N_2, Chem. Eng. J. 327 (2017) 564-572.

[S11] S. Xu, W. C. Li, C. T. Wang, L. Tang, G. P. Hao, A. H. Lu, Self-Pillared Ultramicroporous Carbon Nanoplates for Selective Separation of CH_4/N_2, Angew. Chem. Int. Ed. 60 (2021) 6339-6343.

[S12] W. Su, L. Yao, M. Ran, Y. Sun, J. Liu, X.J. Wang, Adsorption properties of N_2, CH_4, and CO2 on sulfur-doped microporous carbons, J. Chem. Eng. Data 63 (2018) 2914-2920.

[S13] X. F. Wu, B. Yuan, Z. B. Bao, S. G. Deng, Adsorption of carbon dioxide, methane and nitrogen on an ultramicroporous copper metal-organic framework, J. Colloid Interface Sci. 430(2014)78-84.

[S14] P.X. Zhang, J. Wang, W. Fan, Y. Zhong, Y. Zhang, Q. Deng, Z.L. Zeng, S.G. Deng, Ultramicroporous carbons with extremely narrow pore size distribution via in-situ ionic activation for efficient gas-mixture separation, Chem. Eng. J. 375 (2019) 121931.

[S15] T.Y. Li, Y.S. Wang, M.Y. Zhang, B.Y. Liu, Z. Zheng, G.P. Hao, A.H. Lu, Carbon nanofibers with gas selective layer containing rich and accessible ultramicropores for methane/nitrogen separation, Chem. Eng. J. 462 (2023) 142118.

[S16] R. B. Mujmule, M. M. Rajpure, U. Kim, H. Kim, Engineered cellulose-based porous carbon

adsorbents for superior gas adsorption and selective separation of CH_4/H_2 and CH_4/N_2, Sep. Purif. Technol. 327 (2023) 124922.

[S17] S. H. Li, S. G. Fu, Y.Q. Gong, L. Wang, Y. X. Wu, L. Wang, Y. P. Cheng, New insight into efficient CH_4/N_2 separation based on Ni-decorated porous carbon functional composites, Fuel 347 (2023) 128480.

[S18] Y. Zhang, L. Liu, P.X. Zhang, J. Wang, M. Xu, Q. Deng, Z.L. Zeng, S.G. Deng, Ultra-high surface area and nitrogen-rich porous carbons prepared by a low-temperature activation method with superior gas selective adsorption and outstanding supercapacitance performance, Chem. Eng. J. 355 (2019) 309-319.

[S19] J. Wang, R. Krishna, J.F. Yang, S.G. Deng, Hydroquinone and quinone-grafted porous carbons for highly selective CO_2 capture from flue gases and natural gas upgrading, Environ. Sci. Technol. 49 (2015) 9364-9373.

[S20] L.B. Li, J.F. Yang, J.M. Li, Y. Chen, J.P. Li, Separation of CO_2/CH_4 and CH_4/N_2 mixtures by M/DOBDC: A detailed dynamic comparison with MIL-100(Cr) and activated carbon, Micropor. Mesopor. Mat. 198 (2014) 236-246.

[S21] J. L. Hua, T. J. Sun, X. Y. Ren, S. D. Wang, HF-assisted synthesis of ultra-microporous $[Mg_3(OOCH)_6]$ frameworks for selective adsorption of CH_4 over N_2, Microporous Mesoporous Mater. 204 (2015) 73-80.

[S22] Y. Guo, T. J. Sun, Y. M. Gu, X. W. Liu, Q. L. Ke, X. L. Wei, S. D. Wang, Rational Synthesis of Chabazite (CHA) Zeolites with Controlled Si/Al Ratio and Their $CO_2/CH_4/N_2$ Adsorptive Separation Performances, Chem. Asian J.13 (2018) 3222-3230.

[S23] W. C. Zhang, Y. H. Cheng, C. S. Guo, C. P. Xie, Z. H. Xiang, Cobalt Incorporated Porous Aromatic Framework for CO_2/CH_4, Ind.Eng.Chem.Res.57 (2018) 10985-10991.

[S24] R. L. Tang, Q. B. Dai, W.W. Liang, Y. Wu, X. Zhou, H.Y. Pan, Z. Li, Synthesis of novel particle rice-based carbon materials and its excellent CH_4/N_2 adsorption selectivity for methane enrichment from Low-rank natural gas, Chem. Eng. J. 384 (2020) 123388.

[S25] A. A. Niya, T. E. Rufford, Z. H. Zhu, Activated carbon monoliths with hierarchical pore structure from tar pitch and coal powder for the adsorption of CO_2, CH_4 and N_2, Carbon. 103 (2016) 115e124.

[S26] X. H. Shao, Z. H. Feng, R. S. Xue, C. C. Ma, W. H. Wang, X. Peng, D. P. Cao, Adsorption of CO_2, CH_4, CO_2/N_2 and CO_2/CH_4 in Novel Activated Carbon Beads: Preparation, Measurements and Simulation, AIChE J. 57 (2011) 3042-3051.

[S27] Y. Z. Gao, S. Xu, C. T. Wang, X. J. Zhang, R. S. Liu, A. H. Lu, Preparation of molded biomass carbon from coffee grounds and its CH_4/N_2 separation performance, New Carbon Mater. 37 (2022) 1145-1153.